NHH

INSTITUTT FOR FORETAKSØKONOMI

DEPARTMENT OF BUSINESS AND MANAGEMENT SCIENCE

FOR 14 2018

ISSN: 1500-4066

October 2018

Discussion paper

# Flow-Based Market Coupling in the European Electricity Market – A Comparison of Efficiency and Feasibility

BY

**Endre Bjørndal, Mette Bjørndal** AND **Hong Cai**

Norges Handelshøyskole

NORWEGIAN SCHOOL OF ECONOMICS

# Flow-Based Market Coupling in the European Electricity Market – A Comparison of Efficiency *and Feasibility*

Endre Bjørndal[§], Mette Bjørndal[§], Hong Cai[§‡]

*Abstract: In May 2015, the Flow-Based Market Coupling (FBMC) model replaced the Available Transfer Capacity (ATC) model in Central Western Europe to determine the power transfers between countries or price areas. The FBMC model aims to enhance market integration and to better monitor the physical power flows. The FBMC model is expected to lead to increased social welfare in the day-ahead market and more frequent price convergence between different market areas. This paper gives a discussion of the procedures of market clearing and a mathematical formulation of the FBMC model. Moreover, we discuss the relationships between the nodal pricing, ATC, and FBMC models. In addition to an illustrative 3-node example, we examine the FBMC model in two test systems and show the difficulties in implementing the model in practice. We find that a higher social surplus in the day-ahead market may come at the cost of more re-dispatching in real time. We also find that the FBMC model might fail to relieve network congestion and better utilize the power resources, even when compared to the ATC model.*

*Key words: OR in Energy, European power market, Flow-based model, ATC model, Day-ahead market*

## 1. Introduction

Europe has launched the Price Coupling of Regions (PCR) project, which aims at enhancing power exchange between different countries and creating a single European day-ahead market (EIRGRID, 2013). The project has involved a number of power exchanges (PXs), including APX/Belpex, EPEX SPOT, GME, Nord Pool, OMIE, and OTE (NordPool, 2014), accounting for more than 75% of Europe's electricity demand. Currently, most of the European countries rely on the ATC (Available Transfer Capacity) model to process power exchange with other countries. In this model, it is assumed that power can be directly transferred between any two adjacent areas. Only a pre-defined ATC value is used to limit the maximum commercial trading volume

§ Norwegian School of Economics, Helleveien 30, 5045 Bergen, Norway

‡ Corresponding author, Hong.Cai@nhh.no

between two areas (mostly countries) in the day-ahead market. However, as a matter of fact, the alternating current (AC) power flow between any two nodes follows the paths designed by Kirchhoff's laws and is also restricted by the thermal limits of the transmission lines. Therefore, the commercial power transfer is not necessarily equal to the real physical power exchange. Solutions given by the ATC model do not guarantee a congestion-free network. Hence, re-dispatching may be needed, and it incurs extra cost.

In contrast to the ATC model, nodal pricing (Schweppe et al., 1988), reduces the needs for re-dispatching by including all the physical and technical constraints in the market-clearing process. The nodal pricing model has been successfully implemented in many regions and countries, such as Pennsylvania – New Jersey – Maryland (PJM), California, and New Zealand. Within Europe, Poland planned to implement nodal pricing in its domestic market in 2015 and estimated that it would reduce generation cost (Sikorski, 2011). However, this project has been abandoned. In the European context nodal pricing has not been accepted as the standard tool for integrating the European electricity market. One of the main concerns is that nodal pricing might impede market harmonization as it imposes more restrictions (e.g., network capacity constraints) than the ATC model, and thus could limit power exchange between countries.

In recent years, more and more renewable energy has been connected to the power system. This requires more accurate monitoring of power flows, the reason being that installed renewable energy power plants (like wind turbines) are usually located in places without sufficient consumption. Therefore, the utilization of such energy resources often requires long distance transportation, which creates an extra burden for the network and may exacerbate congestion. For example, due to the large wind capacity installation, Germany and its neighboring countries found that their transmission networks had been overloaded more frequently, making their grids less stable and secure (Kunz, 2012). Furthermore, the ATC model may constitute a crude

approximation of real power flows, since the locations of generation plants within a price area do not affect the model solutions and it is assumed that the cheaper power within an area can always be dispatched first. In real-time dispatch, however, physical power follows the laws of physics and it is not necessarily equal to the commercial flow defined by the ATC model. Moreover, Bjørndal et al. (2018) found that when the penetration level of renewable energy is high, applying a low ATC value (i.e., to restrict the commercial power exchange in the day-ahead market) was not sufficient to limit physical power exchange between two connected countries.

In order to better monitor the power flow in an integrated European market, a so called "Flow-Based methodology" Market Coupling (FBMC) was developed by the European TSOs (Schavemaker et al., 2008). Van den Bergh et al. (2016) give a description of the FBMC model. The FBMC model is developed from the nodal pricing model, i.e. the nodal pricing model where we use the power transfer distribution factors (PTDF) to calculate flows. The FBMC model imposes an aggregate (or zonal) PTDF matrix on certain areas/lines in order to limit the power exchange between price areas. Therefore, the solutions given by the FBMC model may still be infeasible in some parts of the network and re-dispatching may be needed. The FBMC model tries to reduce the explicit limitations to cross-border trades, which is an indirect way of dealing with individual line constraints, and instead focuses on selected critical branches (CBs) that are the ones most likely to be influenced by cross-border trading.

In May 2015, Central Western Europe (CWE), a region consisting of the Netherlands, Belgium, France, Luxembourg, and Germany, started to implement the FBMC model. The CWE TSOs have been working on the FBMC calculation method since 2007 and the methodology has been tested with 2-years of off-line parallel runs. The Parallel Run performance report (CASC, 2015) claims that the FBMC model performs better than the ATC model, as it significantly increases the social welfare in the day-ahead market and leads to more frequent price convergence between different market zones, based on the parallel runs results.

Nevertheless, to fully evaluate how the FBMC model works in the European power market, two crucial questions deserve careful examination. First, because the non-CBs are not properly monitored, flows on the non-CBs could affect the accuracy of the FBMC model due to Kirchhoff's loop flow effect, and thus, it is necessary to test to what extent the FBMC model actually helps to relieve the congestion on the CBs. Second, a higher social welfare generally implies that more power is sold/exchanged in the market. However, it is possible that some contracted power in the day-ahead market could not be dispatched in real time due to network limitations. The following re-dispatch may lead to extra cost for the end consumers. Therefore, it is critical to examine whether the increased social welfare in the day-ahead market comes at the cost of more re-dispatching.

The rest of the paper is organized as follows. In section 2, we provide the mathematical formulations of different day-ahead market clearing models (nodal pricing, FBMC, and ATC) as well as the real-time re-dispatch. In section 3, we discuss some formal relationships between the day-ahead market clearing models, illustrated by a 3-node example. Section 4 shows different model results in two numerical examples, a 6-bus test system and the IEEE 24-bus test system. Some conclusions are given in section 5.

## 2. Market procedures and models

### 2.1 Notation

Sets and Indices

| | |
|---|---|
| $i, j \in N$ | Set of nodes |
| $l \in \mathrm{L}$ | Set of directed lines |
| $N_z$ | set of nodes belonging to zone $z$ |
| $CB$ | Set of critical branches |
| $z, zz \in Z$ | Set of price areas |

Parameters

| | |
|---|---|
| $atc_{z,zz}$ | Upper limit on the flows from zone $z$ zone $zz$ |
| $cap_l$ | Thermal capacity limit of the line $l$ |
| $gsk_{i,z}$ | Generation shift keys |
| $nptdf_{l,i}$ | Node to line PTDF matrix |
| $zptdf_{l,z}$ | Zone to line PTDF matrix |

Variables

| | |
|---|---|
| $BEX_{z,zz}$ | The exchange from $z$ to $zz$ |
| ${FL_l}^N$ | Load flow on line $l$ in the nodal pricing model |
| ${FL_l}^{FBMC}$ | Flows on line $l$ in the FBMC model |
| $NEX_z$ | The net position of a zone z |
| $NI_i$ | Net injection at node *i* |
| $Q_i^s$ | Generation quantity (MWh/h) at node *i* |
| $Q_i^d$ | Load quantity (MWh/h) at node *i* |
| $P_i^s$ | Supply curve at node $i$ |
| $P_i^d$ | Demand curve at node $i$ |
| $GUP_i$ | Increased generation at node $i$ |
| $GDN_i$ | Decreased generation at node $i$ |
| $LOADSHED_i$ | Load curtailments at node $i$ |

In this section, we discuss the sequential structure and necessary procedures of day-ahead and real time re-dispatch markets. We also state the mathematical models used in this paper. Generally, three distinct phases can be identified in the operational procedure of FBMC, i.e. pre-market coupling, market coupling and post-market coupling.

### 2.2 Pre-market coupling

Pre-market coupling is the preparation phase where the TSOs prepare the input for the day-ahead market models. The pre-market coupling starts on the evening of Day -2 and lasts until 10:00 on Day -1. For the FBMC model, to prepare the input data, the TSOs

first create one or more base cases, which contain the load and generation information for each bidding zone and the expected state of the detailed grid topology. Given the "base case," the TSOs then will derive the Generation Shift Keys (GSKs), zonal PTDF matrices, Critical Branches (CBs), and other factors. These data are sent to the power exchanges and used as input for the day-ahead market. For the ATC model, the TSOs will assign the maximum trading volume between two connected price areas.

We notice that there might be substantial forecast errors for these input data, as they are collected/generated one or two days before market clearing. The inaccuracy might affect the performance of the day-ahead models in practice. However, in this paper, we do not measure the uncertainty regarding the load, generation, or network topology. We assume that these data are kept unchanged for all the three phases involved.

We further assume that the results given by the nodal pricing model (i.e., the optimal solution and nodal prices) serve as the "base case." The nodal pricing model utilizes all the available resources within the network, and because the FBMC model originates from the nodal pricing model, the nodal pricing results may be considered the best possible estimation for the input data to the FBMC model. Consequently, as the input data in this paper are based on better predictions than what we can expect in practice, the results from the FBMC model may be on the optimistic side.

**Nodal pricing model**

$$\max \sum_i \left[ \int_0^{Q_i^d} P_i^d(Q)dQ - \int_0^{Q_i^s} P_i^s(Q)dQ \right] \tag{1}$$

Subject to:

$$NI_i = Q_i^s - Q_i^d, \forall i \in N \tag{2}$$

$$\sum_i NI_i = 0 \tag{3}$$

$$FL_l{}^N = \sum_i nptdf_{l,i} \cdot NI_i, \forall l \in L \tag{4}$$

$$\left|FL_l{}^N\right| \leq cap_l, \forall l \in L \tag{5}$$

The objective of the nodal pricing model is to maximize the social welfare, i.e., Eq. (1)). Net injection, $NI_i$, to each node $i$ is equal to the difference between generation, $Q_i^s$, and demand, $Q_i^d$, i.e., Eq. (2)). Total generation should be equal to demand (Eq. (3)), i.e. we are not considering losses. The nodal power transfer distribution factor, $nptdf_{l,i}$, which is derived from the lossless DC power flow approximation (Christie et al., 2000), illustrates the linearized impact on line $l$ by injecting 1 MW power at node $i$ and subtracting it from the reference node. The total power flow on line $l$ is given in Eq. (4), and it is restricted by the line thermal capacity limit in Eq. (5).

A generation shift key (GSK) is a factor describing the most probable change in net injection at a node, relative to a change in the net position of the zone that it belongs to (Epexspot, 2011). The set of GSKs is crucial in the FBMC model (De Maere d'Aertrycke and Smeers, 2013). Although the GSKs should be defined before market clearing, in reality they cannot be known until the FBMC calculation is completed. The TSOs calculate the GSKs using a "base case", anticipating grid topology, net positions, and corresponding power flows for each hour of the day of delivery. In practice, a precise procedure to define the GSKs is missing.

In this paper, we define GSKs as the nodal weight of the net position within each zone:[1]

$$gsk_{i,z} = \frac{Q_i^s - Q_i^d}{\sum_{i \in N_z}(Q_i^s - Q_i^d)}, \forall z \in Z, i \in N_z \tag{6}$$

[1] With this approach, the GSKs are not defined in a balanced price area (i.e., where $\sum_{i \in Z}(Q_i^{s*} - Q_i^{d*}) = 0$).

$Q_i^s$ and $Q_i^d$ are unknown before the market clearing, however, we will use the solution given by the nodal pricing model (i.e., $Q_i^{s*}$ and $Q_i^{d*}$) to calculate the GSKs.

Next, TSOs use both GSKs and nodal PTDF matrices to calculate the zonal PTDF matrices, $zptdf_{l,z}$. The zonal PTDF matrices are used to estimate the influence of the net position of any zone on the lines in the FBMC model.

$$zptdf_{l,z} = \sum_{i \in N_z} nptdf_{l,i} \cdot gsk_{i,z}, \forall l \in L, z \in Z \tag{7}$$

$$zptdf_l^{z,zz} = zptdf_{l,z} - zptdf_{l,zz}, \forall l \in L, z \in Z, zz \in Z \tag{8}$$

In the FBMC model, flow restrictions are imposed on selected CBs, and CBs are defined as the transmission lines that are significantly impacted by cross-border trading (JAO.EU, 2014). More specifically, a CB is considered to be significantly impacted by CWE cross-border trades if its maximum CWE zone-to-zone PTDF, $zptdf_l^{z,zz}$ (ref. Eq. (8)), is larger than a fixed threshold value (JAO.EU, 2014). The TSOs publish the CBs and their corresponding Remaining Available Margin (RAM) before market clearing. The RAM is the line capacity that can be used by the day-ahead market. The RAM is calculated as:

$$ram_l = cap_l - F_l' \tag{9}$$

where $cap_l$ is the thermal capacity limit and $F_l'$ includes three components: (1) flows caused by transactions outside the day-ahead market (e.g., re-dispatching, bilateral trades, forward markets), (2) an adjustment value based on TSO knowledge, and (3) a safety margin that is needed to compensate for the approximations and simplifications made by the FBMC model. In the examples in this paper, we simply assume that $ram_l = cap_l$, however it is clear that this way of deciding the RAM leaves a lot of discretion in the hands of the TSOs.

## 2.3 Market coupling[2]

### 2.3.1 FBMC model

$$\max \sum_i \left[ \int_0^{Q_i^d} P_i^d(Q)dQ - \int_0^{Q_i^s} P_i^s(Q)dQ \right] \tag{10}$$

Subject to:

$$NI_i = Q_i^s - Q_i^d, \forall i \in N \tag{11}$$

$$\sum_i NI_i = 0 \tag{12}$$

$$NEX_z = \sum_{i \in N_z} (Q_i^s - Q_i^d), \forall z \in Z \tag{13}$$

$$FL_l{}^{FBMC} = \sum_z zptdf_{l,z} \cdot NEX_z, \forall l \in CB \tag{14}$$

$$\left| FL_l{}^{FBMC} \right| \leq cap_l, \forall l \in CB \tag{15}$$

The objective of the FBMC model is to maximize the social welfare (Eq. (10)). The Net Exchange Position of zone $z$, $NEX_z$, is equal to the difference between the total generation and demand within zone $z$ (Eq. (13)). A positive sign of $NEX_z$ indicates that zone $z$ is a net export area and a negative sign indicates a net import area. The zonal PTDF matrix is applied only to calculate flows on the CBs (Eq. (14)), and these flows are restricted to be less than the thermal capacities (Eq. (15)) (in general, the RAM).

### 2.3.2 ATC model

[2] The models in this section include detailed information about supply and demand in each node, and this is not how these models are formulated in practice. However, the formulations are equivalent to those using zonal aggregates, and convenient in our setting, because we want to compare the different day-ahead models, including the need for re-dispatch, in which case we need the detailed information about supply, demand, and the grid.

$$\max \sum_i \left[ \int_0^{Q_i^d} P_i^d(Q)dQ - \int_0^{Q_i^s} P_i^s(Q)dQ \right] \quad (16)$$

Subject to:

$$NI_i = Q_i^s - Q_i^d, \forall i \in N \quad (17)$$

$$\sum_i NI_i = 0 \quad (18)$$

$$NEX_z = \sum_{i \in N_z} Q_i^s - Q_i^d, \forall z \in Z \quad (19)$$

$$\mathrm{NEX}_z = \sum_{zz} (BEX_{z,zz} - BEX_{zz,z}), \forall z \in Z \quad (20)$$

$$0 \leq BEX_{z,zz} \leq atc_{z,zz}, \forall z, zz \in Z \quad (21)$$

Compared to the FBMC model, the ATC model[3] does not have specific limitations on any selected lines. However, it restricts the total transfer between two price areas to a pre-defined cap, $atc_{z,zz}$, as in Eq. (21). The net position of a zone $\mathrm{NEX}_z$ is equal to the difference of its total export and import (Eq. (20)).

### 2.4 Post-market coupling (re-dispatch model)

Though the FBMC model tries to take the real physical characteristics of the power system into account, it introduces more approximations and simplifications than the nodal pricing model. The zonal PTDF matrices do not accurately represent the characteristics of the power system. The GSKs are based on the prediction of the market-clearing results, which implies that GSKs are subject to forecast errors. It also

[3] In this paper, we do not consider gaming opportunities. However, in reality, it might happen that the producers in a zonal market could bid at a lower price (than the marginal cost) in the day-ahead market to guarantee that their bids are accepted. Then, due to export constraints in the real time, the contracted power in the day-ahead market cannot be dispatched, and the producer will buy back power at a lower price (than the day-ahead price) in the re-dispatch market. This is referred to as the increase-decrease (inc-dec) game, and the producers can profit from this action. It is important to note that the inc-dec game could happen in reality and thus increase the re-dispatching cost (Holmberg and Lazarczyk (2015)).

assumes that any change in the zonal net injection is distributed on the nodes of the zone corresponding to the GSKs. Therefore, the power transfer given by the FBMC model is not equal to the real physical power flow[4], and re-dispatch may be needed in order to obtain a feasible flow in the real network.

We would like to test whether the FBMC model could truly help to relieve the congestion on the CBs. If so, the need for re-dispatch should be reduced. We introduce the re-dispatch model to examine whether the re-dispatch cost will be reduced after applying the FBMC model.

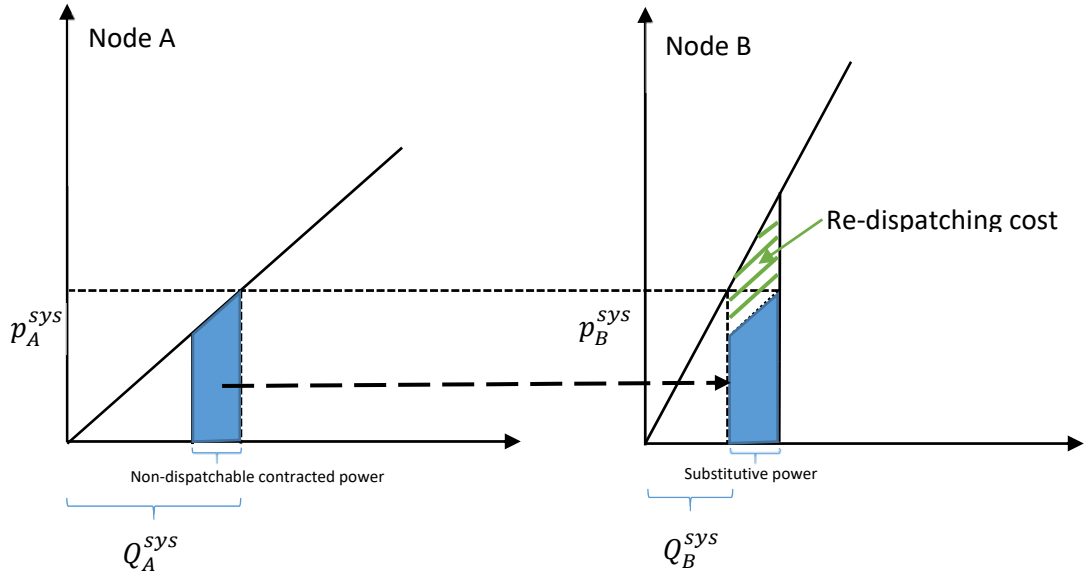


Figure 1: Example of re-dispatch

Figure 1 illustrates the mechanism of the re-dispatch model, using a two-node example where we assume that the prices are equal after the day-ahead market clearing. The day-ahead market determines the clearing price and quantity based on the supply and demand information. The supply curve at node A is less steep than that at node B, which implies that the next unit of power is cheaper at node A. However, we assume that due to network constraints, some of the contracted power at node A cannot be dispatched. Therefore, in order to satisfy the demand, generation at node B has to be increased. We

[4] Although the "base case" in this paper is the solution of the nodal pricing model, the FBMC model is not necessarily converging to the nodal price solution.

assume that the generators bid deviations at their day-ahead marginal cost, i.e. there are no additional cost or restrictions on generation in real time compared to the planning/day-ahead stage, and that there is perfect price discrimination. Generators that cannot dispatch the contracted power, would pay their saved marginal cost to the market, and generators that increase their generation in order to satisfy the demand, would be compensated by their short-run marginal cost of production. This implies that no economic profit is generated from the re-dispatching procedure. The increased generation that replaces the contracted power that cannot be dispatched, is more expensive and leads to an extra cost, which is shown as the area filled with green slashed lines. These assumptions are conservative, and may give a lower re-dispatch cost than what can be expected in practice. In real life, the re-dispatch cost will increase because the generators might bid at a higher price (i.e., marginal price plus the opportunity cost) and because other cost (e.g., start-up cost) and/or restrictions (e.g. inflexible generators) would be taken into account. On the other hand, on the demand side, we assume that day-ahead scheduled load can only be reduced by (costly) loadshedding / load curtailment. In practice, inelastic load may contribute to a more cost-efficient re-dispatch.

$$\min \sum_i \int_{Q_i^{s\prime}}^{Q_i^{s\prime}+GUP_i+GDN_i} P_i^s(Q)dQ + \sum_i voll \cdot LOADSHED_i \tag{22}$$

Subject to:

$$NI_i = \left(Q_i^{s\prime} + GUP_i - GDN_i\right) - (Q_i^{d\prime} - LOADSHED_i), \forall i \in N \tag{23}$$

$$\sum_i NI_i = 0 \tag{24}$$

$$FL_l{}^N = \sum_i nptdf_{l,i} \cdot NI_i, \forall l \in L \tag{25}$$

$$\left|FL_l{}^N\right| \leq cap_l, \forall l \in L \tag{26}$$

$$GUP_i, GDN_i, LOADSHED_i \geq 0, \ \forall i \in N \tag{27}$$

The objective of the re-dispatch model is to minimize total re-dispatch costs (Eq. (22)), including load-shedding, if necessary. The generation, $Q_i^{s\prime}$, and the demand, $Q_i^{d\prime}$, from the day-ahead model are used as input. Generation can be increased by $GUP_i$ or decreased by $GDN_i$. The option to curtail consumer's load ($LOADSHED_n$) is possible only when the feasibility of the re-dispatch model cannot be guaranteed otherwise. We assume that the marginal cost of such an option is significantly higher ($voll \gg 0$) than any other marginal generation cost. The re-dispatch model guarantees that the solution gives feasible flows by applying the nodal PTDF matrix and thermal capacity limits (Eq.(25) and (26)).

## 3. Day-ahead model relationships

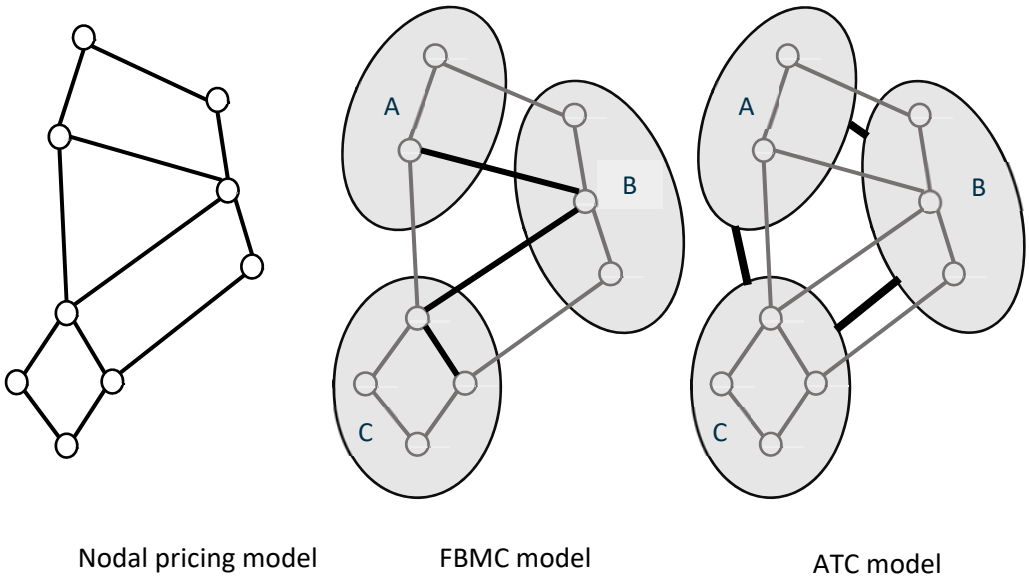


Figure 2: Day ahead market models

Figure 2 gives a brief illustration of different market clearing models. Among the three models, the nodal pricing model needs most detailed information regarding the grid topology. All the elements (i.e., nodes and lines) are taken into account in the model. The laws of physics are applied to the whole network, and line flows are restricted by the thermal capacities. The topology information is only partially used in both the FBMC model and the ATC model. In the FBMC model, the nodes in the grid are divided into several price areas (zones). The laws of physics are only applied to certain

individual lines (i.e., CBs); the other lines (i.e., non-CBs) have no physical restrictions. The CBs could be lines connecting two price areas (i.e., interties) or lines within a price area. In the ATC model, the network is also divided into several price areas. However, instead of using the capacity of individual lines, the ATC model limits power transfer between two price areas to be less than an aggregate capacity (i.e., ATC value). No physical restrictions are applied to lines within a price area. Therefore, within the same area power can be freely traded.

In the following, we further discuss the relationship between these three models in terms of their mathematical formulations. Note from the previous section that the objective functions are the same in all three models. Moreover, since the day-ahead models have linear constraints (based on the linear DC approximation of the AC power flows), the set of feasible solutions in all three formulations are convex.

### 3.1 The nodal pricing model and the FBMC model

Proposition 1:

a) If the GSKs are derived from a feasible solution to the nodal pricing model, then this solution is also feasible in the FBMC model.
b) If the GSKs are derived from an optimal solution to the nodal pricing model, then this optimal solution is feasible also in the FBMC model, and the optimal social surplus of the FBMC model is greater than or equal to the optimal social surplus of the nodal pricing model.
c) If only a subset of lines is selected as CBs, and if $CB_2 \subseteq CB_1 \subseteq L$, then the optimal solution values, $v$, are such that $v_{CB_2}^{fbmc} \geq v_{CB_1}^{fbmc} \geq v_L^{fbmc} \geq v^{nodal}$.

*Proof:*

a) We first assume that the GSKs are derived from a feasible solution to the nodal pricing model (i.e., satisfying Eq. (2)-(5) in Section 2). Let $NI_i{}' = Q_i^{s\prime} - Q_i^{d\prime}$ be the

net nodal injection at node $i$ for the feasible solution to the nodal pricing model, and let $NEX_z' = \sum_{i \in N_z} NI_i'$ for any zone $z$, where $N_z$ is the set of nodes belonging to zone $z$ (we assume that the set of zones is a partition of the nodes of the network, i.e. every node belongs to exactly one zone). A feasible solution to the nodal pricing model must satisfy the capacity constraints, i.e.

$$\left| \sum_i nptdf_{l,i} \cdot NI_i{}' \right| \leq cap_l, \forall l \in L \tag{28}$$

Using Eq. (6) and (7), the zonal PTDFs can be expressed as

$$zptdf_{l,z} = \sum_{i \in N_z} nptdf_{l,i} \cdot \frac{Q_i^{s\prime} - Q_i^{d\prime}}{\sum_{i \in N_z}(Q_i^{s\prime} - Q_i^{d\prime})} = \frac{\sum_{i \in N_z} nptdf_{l,i} \cdot NI_i'}{NEX_z'} \tag{29}$$

If we assume that all lines are CBs in the FBMC model, from (14) and (15) we have that

$$\left| \sum_z zptdf_{l,z} \cdot NEX_z \right| \leq cap_l \quad \forall l \in L \tag{30}$$

Inserting (29) into (30), we get

$$\left| \sum_z \frac{\sum_{i \in N_z} nptdf_{l,i} \cdot NI_i'}{NEX_z'} \cdot NEX_z \right| \leq cap_l \quad \forall l \in L \tag{31}$$

If $NEX_z = NEX_z'$ for all z, then Eq. (31) simplifies to

$$\left| \sum_{i \in \mathrm{N}} nptdf_{l,i} \cdot NI_i' \right| \leq cap_l \quad \forall l \in L \tag{32}$$

which is satisfied for a feasible solution to the nodal pricing model.

b) It follows from a) that if we use an optimal solution to the nodal pricing model to derive the GSKs, then this optimal solution will be feasible in the resulting FBMC

model. Since the objective functions of the two models are the same, the optimal solution of the FBMC model must be at least as good as the optimal solution of the nodal pricing model.

c) The last inequality follows from b). Since the feasible area of the FBMC model is convex, the optimal solution values cannot decrease if we remove constraints from the model formulation.

### 3.2 The nodal pricing model and the ATC model

Proposition 2:

a) If the ATC-capacities, $atc_{z,zz}$, are greater than or equal to the sum of the thermal capacities of the individual lines across the interface, then the ATC model is a relaxation of the nodal pricing model.
b) If the ATC-capacities, $atc_{z,zz}$, are greater than or equal to the sum of the power flow going from zone z to zone zz in the optimal solution to the nodal pricing model, then the optimal social surplus of the ATC model is greater than or equal to the optimal social surplus of the nodal pricing model.

*Proof:*

a) The thermal constraints (i.e., Eq. (5)) imply that the sum of power going from zone z to zone zz is less than or equal to the sum of thermal capacities in any feasible solution to the nodal pricing model. Therefore, if the value of the $atc_{z,zz}$ is set to be greater than or equal to the sum of thermal capacities, any solution that is feasible in the nodal pricing model will also be feasible in the ATC model.

b) If we assume that the value of the $atc_{z,zz}$ is greater than or equal to the sum of power going from zone z to zone zz in the optimal solution to the nodal pricing model, then this solution to the nodal pricing model will always be feasible in the ATC model

(Eq. (16) to (21)). In this case, the ATC model will have an optimal social surplus, which is greater than or equal to the optimal social surplus of the nodal pricing model.

### 3.3 Example network with 3 nodes

We illustrate the relationships between the different congestion management methods for the day-ahead market by using a 3-node example as displayed in Figure 3. The nodes are connected by 3 identical lines (i.e., with the same thermal capacity and admittance). The network is divided into two zones, zone z1 with node 1 and zone z2 with nodes 2 and 3. We let $Q_i$ denote net injection into node $i$, $Q_i > 0$ representing net generation and $Q_i < 0$ representing net withdrawal (demand).

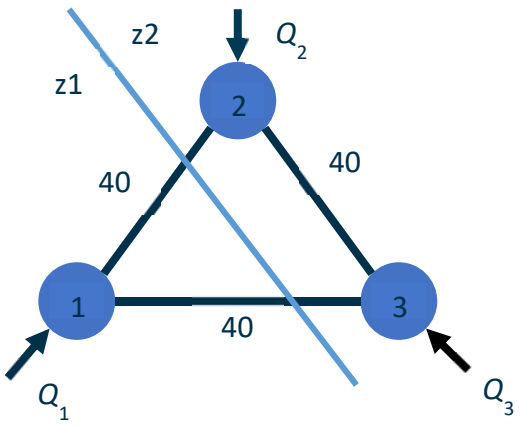


Figure 3: 3-node example

a) Nodal pricing model constraints

We assume node 1 to be the reference node and the corresponding nodal PTDFs are given in Table 1.

| LINE | $nptdf_{l,1}$ | $nptdf_{l,2}$ | $nptdf_{l,3}$ |
|---|---|---|---|
| 21 | 0 | $\frac{2}{3}$ | $\frac{1}{3}$ |
| 31 | 0 | $\frac{1}{3}$ | $\frac{2}{3}$ |
| 23 | 0 | $\frac{1}{3}$ | $-\frac{1}{3}$ |

Table 1: nodal PTDF for the 3-node example

The nodal pricing constraints for the three lines are

$$-40 \leq \tfrac{2}{3}Q_2 + \tfrac{1}{3}Q_3 \leq 40 \quad (33)$$

$$-40 \leq \tfrac{1}{3}Q_2 + \tfrac{2}{3}Q_3 \leq 40 \quad (34)$$

$$-40 \leq \tfrac{1}{3}Q_2 - \tfrac{1}{3}Q_3 \leq 40 \quad (35)$$

b) ATC model constraints

In the ATC model, only the transfer over the interface between the two zones is constrained

$$-ATC \leq Q_2 + Q_3 \leq ATC \quad (36)$$

In practice, setting the ATC transfer capacities between the areas is a challenging task. On the one hand, setting a too high capacity will typically result in infeasible flows, while setting it too low may constrain the system unnecessarily. In the example, we discuss two possibilities: The first is to sum the individual capacities for all the connecting lines (i.e., 80 in our example), and the second is to use a more restrictive value, taking into account the possibility of a "worst case" distribution of supply and demand within the zones (i.e., 60 in our example)[5]. In the example, it seems reasonable to use an ATC value between 60 and 80, however in practice, the ATC transfer limit may be even lower than 60, for instance in order to relieve intra-zonal constraints.

Maximum capacity: $-80 \leq Q_2 + Q_3 \leq 80$ (37)

"Worst case" capacity: $-60 \leq Q_2 + Q_3 \leq 60$ (38)

[5] Since in a zonal pricing context we do not know exactly where supply and demand bids are located, the “worst case” refers to a situation where generation and load is located in the most unfavorable way. In the example, if zone 2 is the exporting zone, the worst possible case is if all net generation was located in one of the nodes 2 or 3. If so, the maximum net generation that is feasible in the nodal model, would be 60 units (⅔ · 60 = 40). Setting the ATC transfer capacity at 60, would then secure that the net transfer is feasible in the nodal model, no matter how generation is distributed over the nodes in zone 2.

c) FBMC model constraints

We follow the procedure described and start by defining the GSKs. For node 1, the GSK is equal to 1, and the PTDFs for zone 1 are zero for all lines. For nodes 2 and 3, the GSKs can be defined as

$$\text{Node 2: } \frac{Q_2'}{Q_2'+Q_3'} = \alpha \tag{39}$$

$$\text{Node 3: } \frac{Q_3'}{Q_2'+Q_3'} = 1-\alpha \tag{40}$$

The PTDFs for zone 2 are then calculated by using the GSKs and the nodal PTDFs

$$zptdf_{21}^{z2} = \frac{1}{3}\cdot\alpha + \frac{1}{3} \tag{41}$$

$$zptdf_{31}^{z2} = -\frac{1}{3}\cdot\alpha + \frac{2}{3} \tag{42}$$

$$zptdf_{23}^{z2} = \frac{2}{3}\cdot\alpha - \frac{1}{3} \tag{43}$$

Assuming all three lines are critical, the FBMC model constraints are the following

$$-RAM_{21} \le (\frac{1}{3}\alpha + \frac{1}{3})\cdot(Q_2+Q_3) \le RAM_{21} \tag{44}$$

$$-RAM_{31} \le (-\frac{1}{3}\alpha + \frac{2}{3})\cdot(Q_2+Q_3) \le RAM_{31} \tag{45}$$

$$-RAM_{23} \le (\frac{2}{3}\alpha - \frac{1}{3})\cdot(Q_2+Q_3) \le RAM_{23} \tag{46}$$

The exact constraints depend on the value of α (the GSKs). However, we also notice that the FBMC model limits the sum of $Q_2$ and $Q_3$, and thus, like the ATC model, is not able to distinguish between the effects of net injections in node 2 versus node 3.

If $\alpha = \frac{1}{2}$ and $RAM_l = cap_l$, then the constraints for the three critical branches are

$$-40 \le \frac{1}{2}\cdot Q_2 + \frac{1}{2}\cdot Q_3 \le 40 \tag{47}$$

$$-40 \le \frac{1}{2}\cdot Q_2 + \frac{1}{2}\cdot Q_3 \le 40 \tag{48}$$

$$-40 \leq 0 \cdot (Q_2 + Q_3) \leq 40 \tag{49}$$

The two first constraints (for lines 21 and 31) are identical and equal to the ATC constraint, with ATC value of 80. The last equation (for line 23) is always satisfied, and not constraining in this case.

If we assume inelastic demand equal to 70 located in node/zone 1, and that the marginal cost for generation is low in node 2 and high in node 3, we obtain the following optimal solutions from the three models:

| | |
|---|---|
| Nodal pricing: | $(Q_1^*, Q_2^*, Q_3^*) = (-70, 50, 20)$ |
| ATC, capacity 80: | $(Q_1^*, Q_2^*, Q_3^*) = (-70, 70, 0)$ |
| ATC, capacity 60: | No solution |
| FBMC: | $(Q_1^*, Q_2^*, Q_3^*) = (-70, 70, 0)$ |

In Figure 4 we show the feasible areas for the different congestion management models, varying the "base case" used to calculate the GSKs and the ATC transfer capacities. Since the energy balance implies that $Q_1 = -(Q_2 + Q_3)$, we only need to consider the $Q_2$ and $Q_3$ variables.

In Figure 4-a, we use $(Q_1', Q_2', Q_3')$ = (−70,70,0) as the "base case", and the ATC transfer capacity is set to 80. We notice that the feasible area of the ATC model covers the feasible points of the nodal pricing model, consistent with the ATC model being a relaxation of the nodal pricing model. The FBMC model on the other hand, includes points that are both feasible and infeasible in the nodal pricing model. Moreover, not all feasible solutions to the nodal pricing model are feasible in the FBMC model. Even if the "base case" is not feasible in neither the nodal pricing model nor the FBMC model, it still generates feasible points in the FBMC model.

In Figure 4-b, the ATC transfer capacity is reduced to 40, and the ATC model is no longer a relaxation of the nodal pricing model.

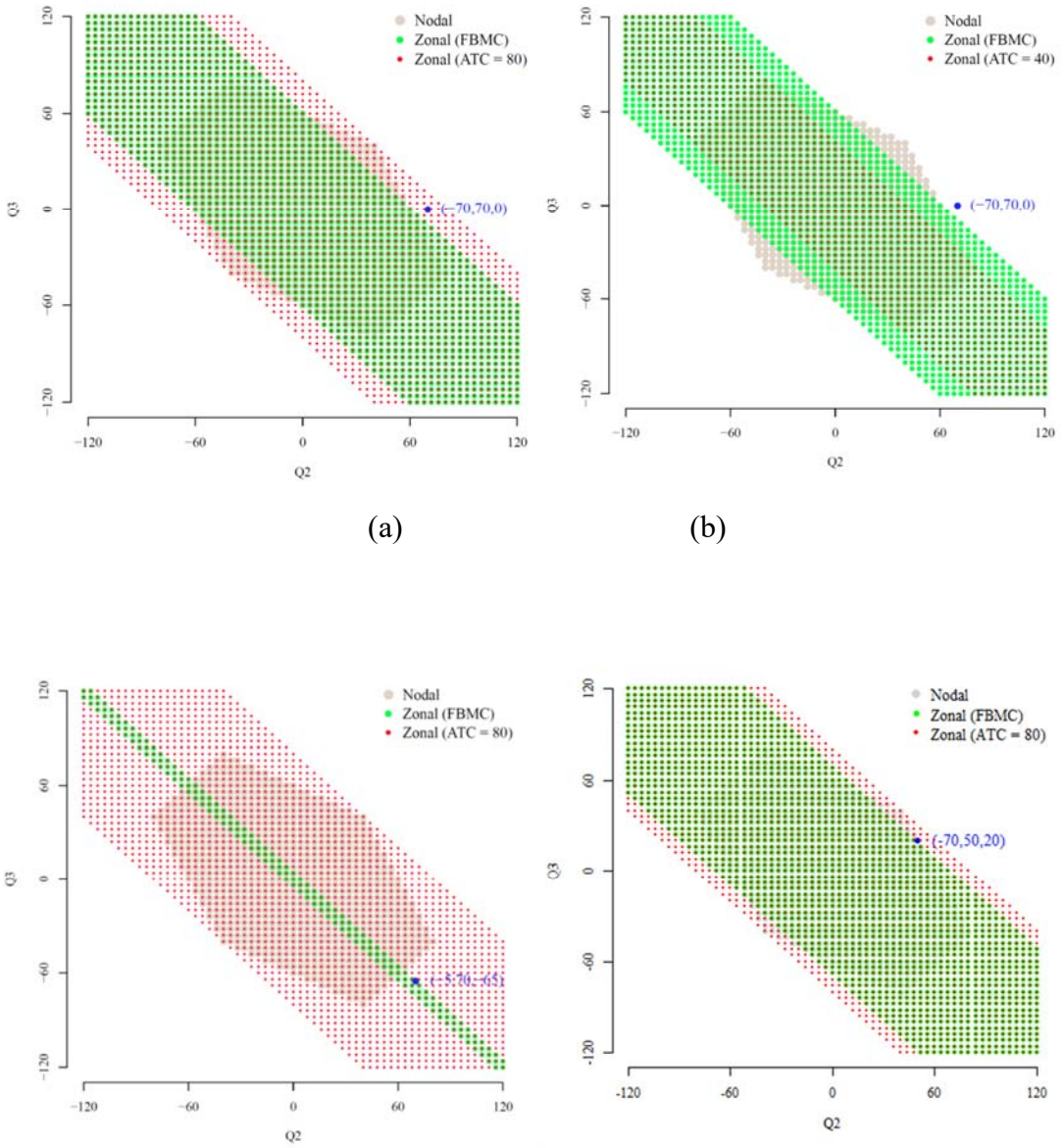


(a) (b)

(c) (d)

Figure 4: Feasible areas of the different dispatch models

In Figure 4-c, we change the "base case" to $(Q_1', Q_2', Q_3') = (-5{,}70, -65)$. The ATC transfer capacity is 80. We find that the feasible area of the FBMC model is very restricted compared to the previous "base case". However, the new "base case" is now included in the feasible area of the FBMC model, showing that nodal feasibility is not a necessary condition for the "base case" to be feasible in the FBMC model.

In Figure 4-d, we use the optimal solution to the nodal pricing model, i.e. $(Q_1', Q_2', Q_3')$ = $(-70,50,20)$, as the "base case". The "base case" is now included in the feasible areas of both the nodal pricing and the FBMC models, consistent with Proposition 1. The figure also illustrates that the FBMC model does not cover the feasible area of the nodal pricing model, showing that the FBMC model is not a relaxation of the nodal pricing model, even if a feasible solution to the nodal pricing model is used as the "base case".

The discussion above regarding the feasible areas of the FBMC model shows the importance of the choice of GSKs.

## 4. Numerical Examples

In this section, we follow the market procedures as discussed in Section 2 in a 6-bus test system as well as the IEEE 24-bus test system (Subcommittee, 1979) to illustrate the impact of the implementation of the FMBC model.

### 4.1 6-bus test system

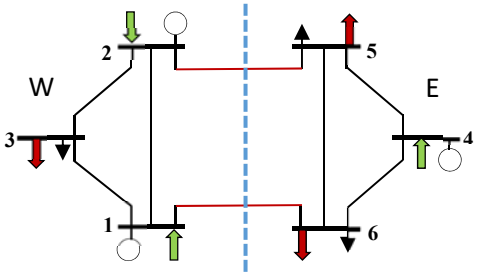


Figure 5: A 6-bus test system

We first consider a 6-bus network example as shown Figure 5. This example is used in Chao and Peck (1998) and de Maere d'Aertrycke and Smeers (2013). Generation is located at buses 1, 2 and 4, while load is located at buses 3, 5 and 6. The supply and demand bids are assumed to be linear in quantity Q, and they are given in Table 2. The parameters regarding the topology are shown in Table 3. The network is divided in a western (W) and eastern (E) zone, as shown in Figure 5.

| *Bus-ID* | *Supply Bids* | *Bus-ID* | *Demand Bids* |
|---|---|---|---|
| 1 | 10+0.05Q | 3 | 37.5-0.05Q |
| 2 | 15+0.05Q | 5 | 75−0.1Q |
| 4 | 42.5+0.025Q | 6 | 80−0.1Q |

Table 2: Bid functions for generation and load for the 6-bus system

| | *From Bus-ID* | *To Bus-ID* | *Area* | *Impedance* | *Capacity* | *Power flow (nodal price solution)* |
|---|---|---|---|---|---|---|
| Line1 | 1 | 2 | W | 1 | 125 | 0 |
| Line2 | 1 | 3 | W | 1 | 125 | 100 |
| Line3 | 1 | 6 | Intertie | 2 | 200 | 200 |
| Line4 | 2 | 3 | W | 1 | 125 | 100 |
| Line5 | 2 | 5 | Intertie | 2 | 250 | 200 |
| Line6 | 4 | 5 | E | 1 | 125 | 100 |
| Line7 | 4 | 6 | E | 1 | 250 | 100 |
| Line8 | 5 | 6 | E | 1 | 125 | 0 |

Table 3: Line parameters

Bus 1 is selected to be the reference node and the node-to-branch PTDF matrix is shown in Table 4. We solve the nodal pricing model and get the net input for each bus. We derive the GSKs as in Eq. (6) to determine the weight for each bus as shown in Table 5.

| | *Bus 1* | *Bus 2* | *Bus 3* | *Bus 4* | *Bus 5* | *Bus 6* |
|---|---|---|---|---|---|---|
| Line1 | 0 | -0.583 | -0.292 | -0.292 | -0.333 | -0.250 |
| Line2 | 0 | -0.292 | -0.646 | -0.146 | -0.167 | -0.125 |
| Line3 | 0 | -0.125 | -0.063 | -0.563 | -0.500 | -0.625 |
| Line4 | 0 | 0.292 | -0.354 | 0.146 | 0.167 | 0.125 |
| Line5 | 0 | 0.125 | 0.063 | -0.438 | -0.500 | -0.375 |
| Line6 | 0 | -0.042 | -0.021 | 0.479 | -0.167 | 0.125 |
| Line7 | 0 | 0.042 | 0.021 | 0.521 | 0.167 | -0.125 |
| Line8 | 0 | 0.083 | 0.042 | 0.042 | 0.333 | -0.250 |

Table 4: Node-to-branch PTDF matrix (Bus 1 is set to be the reference node)

| *Bus-ID* | | *Net Input (nodal price solution)* | *Price (nodal price solution)* | *GSKs* | |
|---|---|---|---|---|---|
| 1 | | 300 | 25 | $\text{gsk}_{1,N}$ | 0.75 |
| 2 | W | 300 | 30 | $\text{gsk}_{2,N}$ | 0.75 |
| 3 | | -200 | 27.5 | $\text{gsk}_{3,N}$ | -0.5 |
| 4 | | 200 | 47.5 | $\text{gsk}_{4,S}$ | -0.5 |
| 5 | E | -300 | 45 | $\text{gsk}_{5,S}$ | 0.75 |
| 6 | | -300 | 50 | $\text{gsk}_{6,S}$ | 0.75 |

Table 5: Generation shift keys

Using the GSKs and the node-to-branch PTDF matrix we calculate the zone-to-branch PTDF matrix (Eq. (7)) given in Table 6. Based on the PTDF matrix, the TSOs then decide on the CBs. We notice that the zone-to-branch PTDF matrix changes as the reference node changes. However, the zone-to-zone PTDF matrix $zptdf_l^{z,zz}$ (Eq. (8)) remains the same even when the reference node changes[6]. The zone-to-zone PTDFs, $zptdf_l^{z,zz}$, could be interpreted as the influence on line $l$ when transferring one unit of power from zone z to zone zz. This also indicates that in practice, the TSOs need to predict on which borders the international transfers happen in order to identify the CBs. This increases the difficulties in implementing the FBMC model.

| | *W* | *E* | *W→E* | *Area* | *CB* |
|---|---|---|---|---|---|
| Line1 | -0.292 | -0.292 | 0 | W | |
| Line2 | 0.104 | -0.146 | 0.25 | W | |
| Line3 | -0.063 | -0.563 | 0.5 | Intertie | *** |
| Line4 | 0.396 | 0.146 | 0.25 | W | |
| Line5 | 0.063 | -0.438 | 0.5 | Intertie | *** |
| Line6 | -0.021 | -0.271 | 0.25 | E | |
| Line7 | 0.021 | -0.229 | 0.25 | E | |
| Line8 | 0.042 | 0.042 | 0 | E | |

Table 6: Zone-to-branch PTDF

CBs are those transmissions lines which are significantly impacted by cross-border trades. We select the lines with the highest values of zone-to-zone PTDFs as the CBs.

[6] This can be proved based on the fact that the sum of GSKs for a zone is constant and equal to 1, and the difference between two nodal PTDFs is the same regardless of the choice of reference node.

In this example, lines 3 and 5 are chosen as the CB candidates. Both lines have the same, highest zone-to-zone PTDF value among all the lines. We test whether these two lines are equally important in the FBMC model. We simulate three cases separately: either of the two CB candidates is chosen as the CB, and both candidates are chosen. The results are given in Table 7. We find that when line 3 is selected as the CB, the solutions are the same regardless of whether line 5 has been chosen or not. The reason is that line 3 is the bottleneck of the system. Power exchange between areas W and E is mainly limited due to the lack of thermal capacity on line 3. Only 400 MW power can be traded between these two areas.

| | *CB=3* | *CB=5* | *CB=3,5* | *Nodal pricing* |
|---|---|---|---|---|
| *Price (W)* | 27.5 | 29.17 | 27.5 | 27.5* |
| *Price (E)* | 47.5 | 45.83 | 47.5 | 47.5* |
| *Social Surplus ①* | 23187.50 | 25020.83 | 23187.50 | 23000 |
| *Re-dispatching cost ②* | 250.95 | 2176.87 | 250.95 | 0 |
| ① - ② | 22936.55 | 22843.96 | 22936.55 | 23000 |
| *W→E(power exchange)* | 400 | 500 | 400 | 400 |
| *Total generation* | 800 | 800 | 800 | 800 |

*Supply volume weighted average price

Table 7: Results for 6-bus system

In the case when only line 5 is selected as the CB, power exchange increases to 500MW. This reduces the price difference and increases the social surplus given in the FBMC model. However, when we take the post-market coupling into account, re-dispatching cost increases significantly. We re-calculate the social surplus by subtracting the re-dispatching cost. We find that this case has the lowest social surplus when taking into account the re-dispatch cost.

This example shows the importance of choosing the "right" CBs before market clearing in the FBMC model. Based on the zone-to-zone PTDF matrices, both lines 3 and 5 show equal importance in terms of inter-zonal trading. However, the results reveal that line 3 is actually more important. If only line 5 is selected, a higher re-dispatch cost

occurs, which leads to lower social surplus. In such a case, the end-consumers might have to bear the cost.

We further compare the FBMC model to the ATC model. We set the ATC value to 400 MW in the ATC model. That is to limit the maximum trading volume between W and E to 400 MW (the total capacity for the interties is 450 MW). We find that the solutions are exactly the same for both the ATC and FBMC models. This indicates that the FBMC model does not necessarily outperform the ATC model in terms of relieving the congestion on the CBs in this example.

Both the ATC model[7] and the FBMC model give a higher objective function value than the nodal pricing model (see Proposition 1 and 2). However, after taking the re-dispatch cost into account, the nodal pricing model gives the highest social surplus.

### 4.2 The IEEE 24-bus test system

| *Bus-ID* | *Supply Bids* | *Bus-ID* | *Demand Bids* |
|---|---|---|---|
| 1 | 15.483+0.0150q | 2 | 65.000−0.0820q |
| 4 | 20.000+0.0161q | 3 | 75.517−0.1129q |
| 7 | 12.555+0.0352q | 5 | 63.000−0.0925q |
| 11 | 29.000+0.0362q | 6 | 42.289−0.0847q |
| 13 | 39.859+0.1012q | 8 | 62.517−0.1016q |
| 15 | 29.678+0.0220q | 9 | 50.517−0.0876q |
| 17 | 23.180+0.0295q | 10 | 59.517−0.0502q |
| 21 | 30.031+0.0270q | 13 | 45.289−0.0733q |
| 22 | 20.966+0.0268q | 14 | 64.517−0.0851q |
| 23 | 35.330+0.0552q | 16 | 58.289−0.1146q |
| | | 18 | 76.547−0.0792q |
| | | 19 | 72.517−0.0682q |
| | | 20 | 63.289−0.1033q |
| | | 24 | 72.289−0.0733q |

Table 8: Bid functions of generation and load for IEEE24 system

[7] The total volume of power transfer between the two price areas is the same in both the ATC and the nodal pricing models.

We next apply the FBMC model to the IEEE 24-bus test system with topology shown in Figure 6. The supply and demand bid functions are derived from Deng et al. (2010) and shown in Table 8. Generators are located at buses 1, 4, 7, 11, 13, 15, 17, 21, 22 and 23. Loads are at the rest of the buses.

Previous research shows that in order to properly implement the ATC model, a zone should be aggregated in such a way that congestion seldom happens within the zone. This might also be a critical issue in the FBMC model. However, in the European power market, most of the price areas are currently defined according to the national boundaries. Therefore, we do not study how to partition the nodes in this IEEE 24-bus system. We arbitrarily divide the system into two areas S and N. The S area contains buses 1 to 10 and the N area contains buses 11 to 24. We follow the same procedure as we demonstrated in the 6-bus system to find the CBs. We choose 6 lines (the red lines in Figure 6) which are considered to be most affected by cross-border trades indicated by the zone-to-zone PTDF matrix.

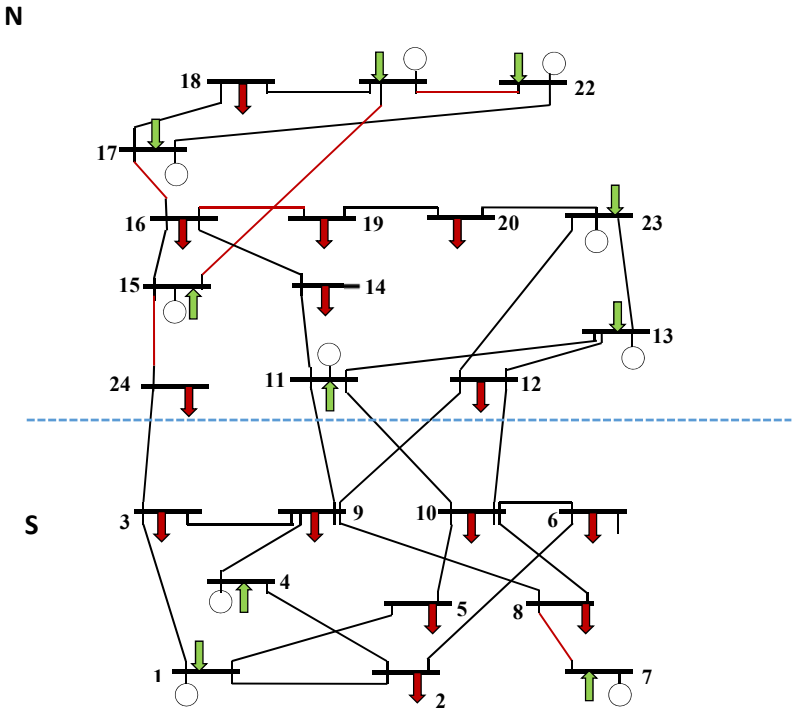


Figure 6: IEEE 24 network

As shown in Table 9, compared to the nodal pricing model, the FBMC model has a higher social surplus (i.e., objective value) as indicated by Proposition 1. However, the cost per unit of electricity that a customer pays could be much higher if the re-dispatch cost is taken into account. The power in the N area is generally cheaper than that in the S area. Due to the effect of Kirchhoff's law however, the power flow goes from the S area (high-price area) to the N area (low-price area) in the nodal pricing model, i.e. an example of an "adverse" flow that is optimal. However, this is not the case in neither the FBMC model nor the ATC model. Here power flows from the N area (low-price area) to the S area (high-price area) regardless of Kirchhoff's laws, and even if this seems more intuitive, it is not optimal. Therefore, the FBMC model is not working as well as the nodal pricing model in terms of following the physical constraints. This example also shows that proper partitioning of zones is an important issue to study even when implementing the FBMC model.

| | *ATC* | *FBMC* | *Nodal pricing* |
|---|---|---|---|
| *Price (N)* | 34.205 | 33.994 | 24.313* |
| *Price (S)* | 37.314 | 37.444 | 38.941* |
| *Social Surplus ($)* | 104165 | 104044 | 90273 |
| *Re-dispatching cost ($) (Gernetation part)* | 14353 | 14099 | 0 |
| *Load shedding (MW)* | 202 | 207 | 0 |
| *N→S (power exchange)(MW)* | 380 | 343 | -343 |
| *Unit cost* | 32.229 | 32.232 | 28.464 |

*Supply volume weighted average price

Table 9: Results for IEEE24 system

We then compare the FBMC results to the ATC model in which the ATC value is set to 380 MW. We find that the net inter-zonal power exchange is 343 MW in the FBMC model compared to 380 MW in the ATC model. Moreover, the average cost for each unit power is slightly higher in the FBMC model. We further check the physical power flow given by solutions to the day-ahead markets. We use Eq. (4) to calculate the physical power flow by fixing the value of nodal load and generation given by the day-

ahead market models (i.e., ATC and FBMC models). From the results in Table 10, we notice that 3 out of 6 selected CBs are congested in both the ATC and FBMC models. Thus, in this example, applying the FBMC model does not help these lines to become congestion-free. We even find that two of the three lines become more congested in the FBMC model than in the ATC model.

| | *From* | *To* | *Line Capacity* | *Actual Flow (ATC)* | *Actual Flow (FBMC)* |
|---|---|---|---|---|---|
| *CB 1* | 7 | 8 | 350 | 615 | 609 |
| *CB 2* | 15 | 21 | 1000 | -353 | -360 |
| *CB 3* | 15 | 24 | 500 | 392 | 400 |
| *CB 4* | 16 | 17 | 500 | -510 | -519 |
| *CB 5* | 16 | 19 | 500 | 537 | 543 |
| *CB 6* | 21 | 22 | 500 | -366 | -369 |

Table 10: Actual flow for CBs

## 5. Conclusions

In this paper we discuss the FBMC model, which has recently been implemented in parts of the European electricity market. We illustrate the relationships between the various congestion management models in a 3-node example, and further test the FBMC model in a 6-bus system, as well as the IEEE 24-bus test system. In the paper we simplify the model to a great extent by neglecting the uncertainties regarding the load, generation, and network topology. However, we still find results showing that it is difficult to implement the FBMC model appropriately. Therefore, it might be a great challenge to apply the FBMC model in the current European power system.

We find it difficult to identify the CBs simply based on the zonal PTDF matrix. It requires that the TSOs forecast directions of the cross-border power exchange. Moreover, the TSOs might choose the wrong CBs based on the information given by the zonal PTDF matrix. In our example, a higher social surplus in the day-ahead market could occur if CBs are not correctly defined. However, this selection leads to a high re-dispatch cost in the post market coupling. This could do harm to the end-consumers as

they might have to bear the high re-dispatch cost. We also find that the FBMC model does not necessarily outperform the ATC model in terms of helping to relieve the congestion and to better utilize the resources within the network.

We find that price areas are currently defined according to the national boundaries in the European power market, and that this might lead to power being exchanged in the wrong direction. This happens not only in the ATC model, but also in the FBMC model. This is an important issue to study when implementing the FBMC model.

**Reference**


[1] Endre Bjørndal, Mette Bjørndal, Hong Cai, Evangelos Panos, Hybrid pricing in a coupled European power market with more wind power, In European Journal of Operational Research, Volume 264, Issue 3, 2018, Pages 919-931, ISSN 0377-2217

[2] CASC 2015 CWE Flow Based Market- coupling project: Parallel Run performance report http://www.casc.eu/media/Parallel%20Run%20performance%20report%2026-05-2015.pdf

[3] Chao, Hung-po, and Stephen C. Peck. "Reliability management in competitive electricity markets." Journal of Regulatory Economics 14.2 (1998): 189-200.

[4] Christie, Richard D., Bruce F. Wollenberg, and Ivar Wangensteen. "Transmission management in the deregulated environment." Proceedings of the IEEE 88.2 (2000): 170-195.

[5] de Maere d'Aertrycke G., Smeers Y. (2013) Transmission Rights in the European Market Coupling System: An Analysis of Current Proposals. In: Rosellón J., Kristiansen T. (eds) Financial Transmission Rights. Lecture Notes in Energy, vol 7. Springer, London

[6] Deng, Shi-Jie, Shmuel Oren, and A. P. Meliopoulos. "The inherent inefficiency of simultaneously feasible financial transmission rights auctions." Energy Economics 32.4 (2010): 779-785

[7] EIRGRID (2013). "Price Coupling of Regions (PCR) initiative and the North West Europe (NWE) project." EirGrid, 2013. http://www.eirgrid.com/media/PCR_NWE_MO_TSO_Review.pdf

[8] Epexspot (2011), "CWE_Flow_Based_Questions_and_Answers" https://www.epexspot.com/document/14065/CWE_Flow_Based_Questions_and_Answers.pdf

[9] Holmberg, Pär, and Ewa Lazarczyk. "Comparison of congestion management techniques: Nodal, zonal and discriminatory pricing." Energy Journal 36, no. 2 (2015): 145-166.

[10] JAO.EU (2014) "Documentation of the CWE FB MC solution As basis for the formal approval-request." JAO.EU, 2014

[11] Kunz, Friedrich. "Managing Congestion and Intermittent Renewable Generation in Liberalized Electricity Markets." Dissertation 2012.

[12] Nordpool (2014), "4M Market Coupling launches successfully by using PCR solution." http://www.nordpoolspot.com/globalassets/download-center/pcr/pcr-pr_4m-mc-launch.pdf

[13] Van den Bergh, Kenneth, Jonas Boury and Erik Delarue, The Flow-Based Market Coupling in Central Western Europe: Concepts and definitions, In The Electricity Journal, Volume 29, Issue 1, 2016, Pages 24-29, ISSN 1040-6190

[14] Schavemaker, P.H., et al., "Flow-based allocation in the Central Western European region", paper C5-307, CIGRE, 2008.

http://citeseerx.ist.psu.edu/viewdoc/download?doi=10.1.1.459.7550&rep=rep1&type=pdf

[15] Schweppe F C, Tabors R D, Caraminis M C, et al. "Spot pricing of electricity." 1988.

[16] Sikorski, Tomasz. "Nodal pricing project in Poland." 4th IAEE International Conference: Institutions. Efficiency and Evolving Energy Technologies. Stockholm, 2011.

[17] Subcommittee, P. M. "IEEE reliability test system." IEEE Transactions on Power Apparatus and Systems (1979): 2047-2054.